Solid State Communications 177 (2014) 16–19

Contents lists available at ScienceDirect

Solid State Communications

journal homepage: www.elsevier.com/locate/ssc

Microstructural and vibrational properties of PVT grown Sb_2Te_3 crystals

K.A. Kokh [a,b], V.V. Atuchin [c,*], T.A. Gavrilova [d], N.V. Kuratieva [e], N.V. Pervukhina [e], N.V. Surovtsev [f]

[a] Laboratory of Crystal Growth, Institute of Geology and Mineralogy, SB RAS, Novosibirsk 630090, Russia
[b] Department of Mineralogy and Petrography, Novosibirsk State University, Novosibirsk 630090, Russia
[c] Laboratory of Optical Materials and Structures, Institute of Semiconductor Physics, SB RAS, Novosibirsk 630090, Russia
[d] Laboratory of Nanodiagnostics and Nanolithography, Institute of Semiconductor Physics, SB RAS, Novosibirsk 630090, Russia
[e] Laboratory of Crystal Chemistry, Institute of Inorganic Chemistry, SB RAS, Novosibirsk 630090, Russia
[f] Laboratory of Condensed Matter Spectroscopy, Institute of Automation and Electrometry, SB RAS, Novosibirsk 630090, Russia

ARTICLE INFO

Article history:
Received 27 August 2013
Accepted 15 September 2013
by E.L. Ivchenko
Available online 24 September 2013

Keywords:
A. Sb_2Te_3
B. PVT growth
C. Crystal structure
E. Raman spectroscopy

ABSTRACT

High-quality Sb_2Te_3 microcrystals have been grown by the physical vapor transport (PVT) method without using a foreign transport agent. The microcrystals grown under optimal temperature gradient are well facetted and they have dimensions up to ~200 μm. The phase composition of the grown crystals has been identified by the X-ray single crystal structure analysis in space group $R-3m$, $a=4.2706(1)$, $b=30.4758(8)$ Å, $Z=3$ ($R=0.0286$). Raman microspectrometry has been used to describe the vibration parameters of Sb_2Te_3 microcrystals. The FWHM parameters obtained for representative Raman lines at 69 and 111 cm^{-1} are as low as 5 and 8.6 cm^{-1}, respectively.

1. Introduction

Antimony telluride, Sb_2Te_3, is related to tetradymite-type crystals with general composition A_2B_3 (A=Bi, Sb; B=S, Se, Te) whose crystal structure belongs to trigonal space group $R-3m$. For many years, this telluride has been actively studied for very good thermoelectric properties [1–4]. A wide range of the solid solutions and composites based on Sb_2Te_3 has been prepared and evaluated to see and improve the structural, electrical and mechanical parameters needed for industrial applications in thermoelectric devices [2,5–11]. Besides, for several recent years Sb_2Te_3 has been of great interest because of topological insulator properties [12–15]. The formation of A_2B_3 crystals with high-quality structure is of prime importance for comparative diagnostics of thin films and nanostructures fabricated by epitaxial and chemical synthesis techniques [16–21]. It is well known that low-defect crystals with dimensions up to the mm range can be grown with the help of the physical vapor transport (PVT) method, if vapor pressure of the source material is high enough at growth temperatures [22–25]. Typically, the vapor transport grown microcrystals are well facetted, and, specifically for tetradymite family compounds, the plate-like crystals with the atomically flat (0001) surface can be grown [21,24–28]. In the present study, the Sb_2Te_3 microcrystals are grown by the physical vapor transport (PVT) method, and the structural and vibrational properties of the microcrystals are explored.

2. Experimental

High purity (4 N) elementary Sb and Te were used for the charge preparation. The growth experiment was performed in a fused silica ampoule of 15 mm in diameter and 300 mm long, initially etched with HF–HNO_3 acid mix and rinsed with bidistilled water. The element charge of 15 g weighted in stoichiometric composition of Sb:Te=2:3 was fused in the ampoule sealed at residual pressure ~10^{-4} bar. The sealed ampoule was placed in a single zone horizontal furnace to obtain the synthesized Bi_2Te_3 compound by the technique described elsewhere [29]. After synthesis, the ampoule was inclined so that the melt was located in the high temperature part of the ampoule, while the opposite end was at the temperature below the melting point of Sb_2Te_3 (902 K). The Sb_2Te_3 melt was taken as a vapor source because, earlier, it was reported that, at low source temperatures $T<400$ °C, the tellurium nanocrystals are growing instead of Sb_2Te_3 because of tellurium dominance in the vapor [27]. Besides, the equilibrium vapor pressure over solid Sb_2Te_3 is comparatively low, and vaporization appeared by molecular forms of Sb_2Te_2, Te_2 and SbTe [30]. Using Sb_2Te_3 melt as a source increases the total vapor pressure and provides the parallel evaporation of Sb and Te, supposedly, in atomic forms.

* Corresponding author. Tel.: +7 383 3308889; fax: +7 383 3332771.
E-mail address: atuchin@isp.nsc.ru (V.V. Atuchin).

0038-1098/$ - see front matter © 2013 Elsevier Ltd. All rights reserved.
http://dx.doi.org/10.1016/j.ssc.2013.09.016

The precipitation of microcrystals occurred in the opposite part of the ampoule located in the cold zone (~820 K). The growth experiment lasted for ~20 h. Then, the furnace was slowly cooled down to the room temperature at the rate of 20 K/h and the ampoule was cracked to get the silica pieces covered with Bi_2Te_3 microcrystals. The resulting PVT-grown dark plate-like crystals were up to 1 mm in size.

Micromorphology of the crystals formed on the ampoule walls was observed by SEM using LEO 1430 device. The microplates grown were well facetted. Chemical composition of the microplates was estimated with EDX measurements. The phase composition of grown crystals was identified by X-ray single crystal structure analysis. X-ray intensity data were collected on a Bruker X8Apex CCD diffractometer using standard techniques (ω- and φ-scans of narrow frames) and corrected for absorption effects (SADABS) [31]. The structure was solved with direct methods [32] and refined by full-matrix least-squares on F^2 using the SHELX97 program set [33]. Crystallographic data and details of single crystal diffraction experiments for the compound are given in Table 1. All atoms were refined anisotropically (Table 2).

Room temperature Raman scattering experiment was carried out in back-scattering geometry with a triple grating spectrometer TriVista 777 under illumination by the lines of λ=532 nm of a solid-state laser and λ=633 nm from He–Ne laser. An achromatic lens with the focal length of 60 mm was used for focusing laser beam and collecting scattering light. The low laser power of 15 mW was used, and it was verified that, under the conditions of our focusing system, this power does not affect the sample. Wavelength scale calibration of the spectrometer was produced in reference to the spectrum of a neon-discharge lamp. The spectral resolution during measurements was ~2.5 cm^{-1} (FWHM). Raman spectra were recorded without polarization selection. Experimental spectra were corrected for the dark count contribution and for the contribution of low-frequency Raman scattering from the air.

Table 1
Crystal data and structure refinement for Sb_2Te_3.

Empirical formula	Sb_2Te_3
Formula weight	626.30
Crystal system	Rhombohedral
Space group	$R-3m$
Unit cell dimensions	a=4.2706(1) Å
	c=30.4758(8) Å
	γ=120°
V	481.35(2) Å^3
Z	3
Density (calculated)	6.482 mg/m^3
Absorption coefficient	21.639 mm^{-1}
F(000)	774
Crystal size	0.22 × 0.16 × 0.02
Theta range for data collection	5.67°–32.57°
Index ranges	$-6 \le h \le 3, -7 \le k \le 6, -45 \le l \le 45$
Reflections collected	1929
Independent reflections	265 (R_{int}=0.0548)
Completeness to θ=25.00°	95.7%
Max. and min. transmission	0.649 and 0.022
Refinement method	Full-matrix least-squares on F^2
Data/restraints/parameters	265/0/10
Goodness-of-fit on F^2	1.161
Final R indices ($I > 2\sigma_I$)	R_1=0.0286, wR_2=0.0701
R indices (all data)	R_1=0.0289, wR_2=0.0707
Extinction coefficient	0.0197(12)
Largest diff. peak and hole	2.211 and −1.789 e/Å^3

Table 2
Atomic coordinates (×10^4) and equivalent isotropic displacement parameters (Å^2 × 10^3) for Sb_2Te_3. U_{eq} is defined as one-third of the trace of the orthogonalized U_{ij} tensor.

Atom	x	y	z	U_{eq}
Sb(1)	0	0	3986(1)	18(1)
Te(1)	0	0	0	12(1)
Te(2)	0	0	7878(1)	14(1)

3. Results and discussion

The SEM images of grown crystals are shown in Fig. 1. The individual druses of well-facetted plate-like crystals were found on the internal surface of dissected silica ampoule. As a rule, the druses were clamped to the ampoule wall by a small area bottom spot and can be easily separated without damage. The selected plate crystals were as large as 50–200 μm in diameter. As is evident from Fig. 1(b), the growth proceeds by layer-by-layer mechanism with the formation of flat low-growth-rate facets. This is typical growth behavior for the layered structure crystals with high volatility [25,26,34–36]. The EDX measurements made for three crystals yield the element content ratio Sb:Te=0.68–0.70 that is in good relation with nominal composition Sb:Te=0.67 of Sb_2Te_3. Thus, the micromorphology and element content in the microplates verify the formation of Sb_2Te_3 crystals.

To reveal the phase composition of the grown crystals, the crystal structure was determined for selected facetted microcrystals.

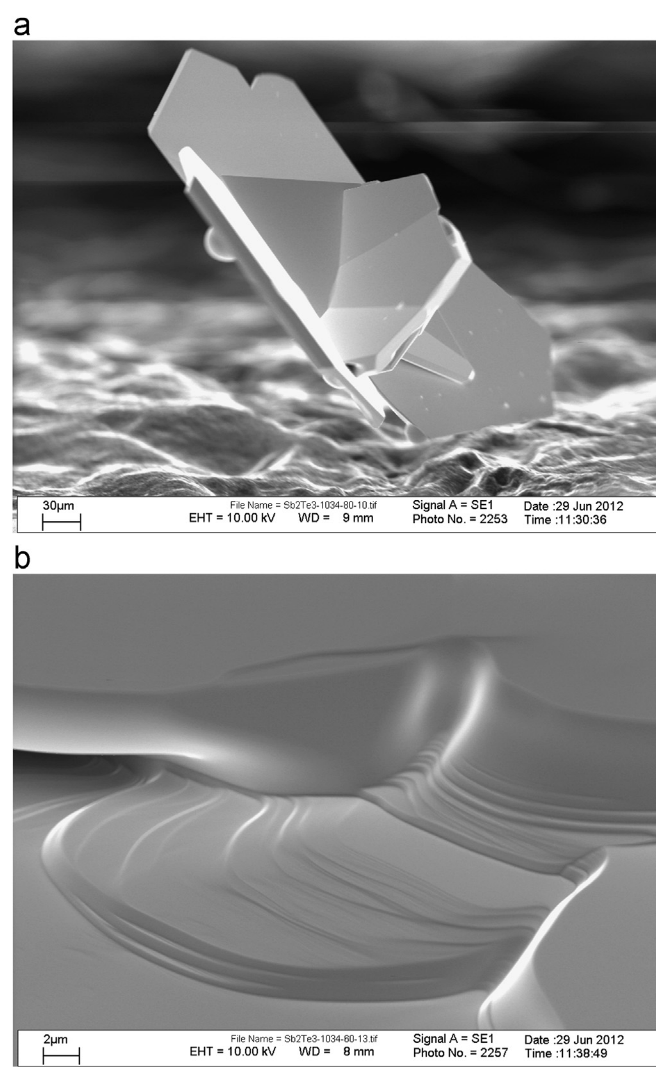

Fig. 1. SEM images of (a) individual Sb_2Te_3 crystal clamped on the adhesive tape surface and (b) echelons of the growth terraces.

The crystallographic data and details of single crystal diffraction experiments produced for Sb_2Te_3 are given in Table 1. The atomic coordinates are given in Table 2. The values shown in Table 2 are in good relation with the earlier results reported for Sb_2Te_3 [37,38]. The layered crystal structure of Sb_2Te_3 is illustrated in Fig. 2 [39]. The unit cell parameters available in literature for Sb_2Te_3 are collected in Table 3. A comparatively narrow possible variation range ~0.2% is found for parameter *a*. Contrary to that, the variation of parameter *c* may be as high as 2% depending on the sample preparation and real defective structure. It should be pointed, however, that the strong variation of parameter *c* is governed by very low value obtained in Ref. [38]. Excluding this result, the possible variation range of parameter *c* is also as narrow as ~0.2%. So, the unit cell parameters of Sb_2Te_3 seem to be relatively stable in reference to the defect formation.

An example of Raman spectrum recorded from a microcrystal studied under the excitation at $\lambda = 633$ μm is shown in Fig. 3. The lines observed at 69, 111 and 165 cm^{-1} are well related to A_{1g} and E_g modes of Sb_2Te_3 [21,41–43]. The apparent line width of the modes at 69 and 111 cm^{-1} is 5 and 8.6 cm^{-1}, respectively (FWHM, without correction to the spectral width used in the experiment). The dominance of the lines at 83, 117, 139, 190 and 254 cm^{-1}, however, was found when the light at $\lambda = 532$ nm was used for the excitation at a higher power. The spectral features at 83, 117, 139 cm^{-1} can be attributed to tellurium segregated at the surface [44,45]. The lines at 190 and 254 cm^{-1} seem to be related to Sb_2O_3 [44]. Thus, a strong modification of the Sb_2Te_3 surface is possible under short-wavelength laser illumination.

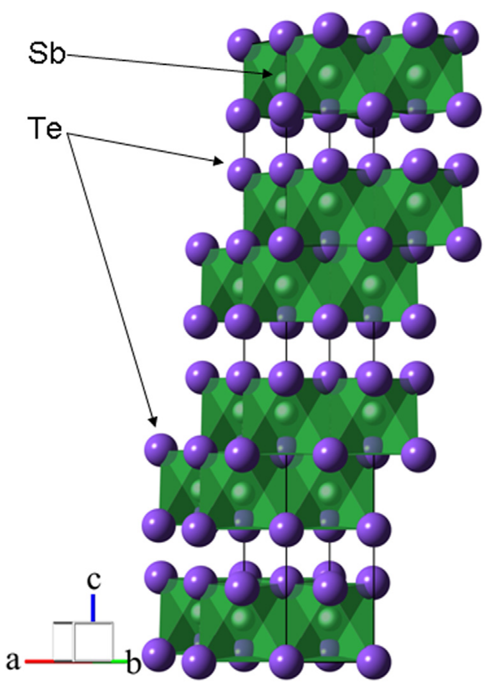

Fig. 2. (Color online) Crystal structure of Sb_2Te_3. The unit cell is outlined. Lone atoms are omitted for clarity.

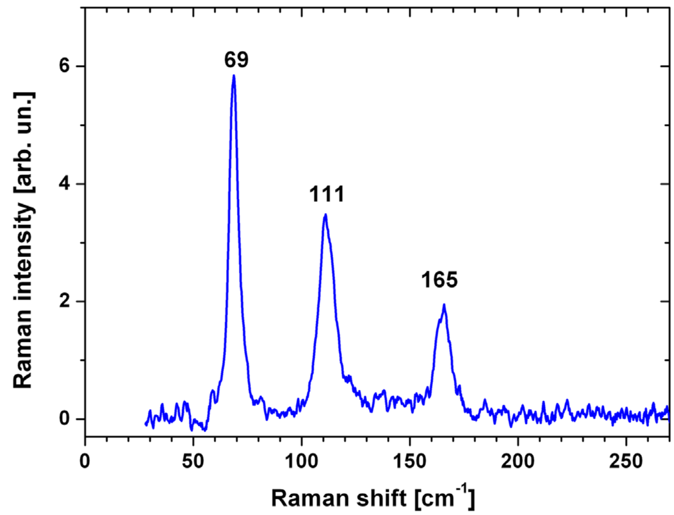

Fig. 3. (Color online) Raman spectrum recorded under excitation at $\lambda = 633$ μm.

Table 3
Unit cell parameters of Sb_2Te_3.

a (Å)	*c* (Å)	Ref.
4.275	30.490	[5]
4.264(1)	30.4580(70)	[37]
4.271	29.877	[38]
4.2654	30.4438	[40]
4.2706(1)	30.4758(8)	This study

4. Conclusions

Thus, the sublimation of Sb_2Te_3 melt in vacuum can be successfully used for fabrication of high-quality plate like Sb_2Te_3 single crystals with the dimensions large enough for detailed observation of physical properties of this technologically valuable telluride. The crystals are of high structural quality and have a developed (0001) surface suitable for physical parameter measurements as it is verified by single crystal structure analysis and Raman scattering experiment. Thus, such Sb_2Te_3 microcrystals can be used as a reference for the comparative observation of Sb_3Te_3-based films and nanostructures including doping systems.

Acknowledgments

This study is supported by the Ministry of Education and Science of the Russian Federation (Contract 16.518.11.7091) and RAS Presidium through Fundamental Research Program 8.

Appendix A. Supplementary materials

Supplementary data associated with this article can be found in the online version at http://dx.doi.org/10.1016/j.ssc.2013.09.016.

References

[1] C.J. Vineis, A. Shakouri, A. Majumdar, M.G. Kanatzidis, Advanced Materials 22 (2010) 3970–3980.
[2] V.A. Kulbachinskii, V.G. Kytin, A.A. Kudryashov, P.M. Tarasov, Journal of Solid State Chemistry 193 (2012) 47–52.
[3] Ming Tan, Yuan Deng, Yao Wang, Journal of Nanoparticle Research 14 (2012) 1204.
[4] L.P. Bulat, V.B. Osvenskii, Y.N. Parkhomenko, D.A. Pshenai-Severin, Physics of the Solid State 54 (11) (2012) 2165–2172.
[5] B.M. Goltzman, V.A. Kudinov, I.A. Smirnov, Semiconductor Thermoelectric Materials on the Basis of Bi_2Te_3, Nauka, Moscow, 1972.
[6] Z. Bastl, I. Spirovova, M. Janovska, Collection of Czechoslovak Chemical Communications 62 (2) (1997) 199–212.
[7] A. Datta, J. Paul, A. Kar, A. Patra, Z.L. Sun, L.D. Chen, J. Martin, G.S. Nolas, Crystal Growth and Design 10 (2010) 3983–3989.
[8] Cheng Peng, Liangcai Wu, Zhitang Song, Feng Rao, Min Zhu, Xuelai Li, Bo Liu, Limin Cheng, Songlin Feng, Pingxiong Yang, Junhao Chu, Applied Surface Science 257 (2011) 10667–10670.

[9] Sima Aminorroaya-Yamini, Chao Zhang, Xiaolin Wang, Ivan Nevirkovets, Journal of Physics D: Applied Physics 45 (2012) 125301.
[10] V.D. Blank, S.G. Buga, V.A. Kulbachinskii, V.G. Kytin, V.V. Medvedev, M.Y. Popov, P.B. Stepanov, Physical Review B 86 (7) (2012) 075426.
[11] L.D. Ivanova, L.I. Petrova, Y.V. Granatkina, V.G. Leontyev, A.S. Ivanov, S.A. Varlamov, Y.P. Prilepo, A.M. Sychev, A.G. Chuiko, I.V. Bashkov, Inorganic Materials 49 (2) (2013) 120–126.
[12] D. Hsieh, Y. Xia, D. Qian, L. Wray, F. Meier, J.H. Dil, J. Osterwalder, L. Patthey, A.V. Fedorov, H. Lin, A. Bansil, D. Grauer, Y.S. Hor, R.J. Cava, M.Z. Hasan, Physical Review Letters 103 (14) (2009) 146401.
[13] Haijun Zhang, Chao-Xing Liu, Xiao-Liang Qi, Xi Dai, Zhong Fang, Shou-Cheng Zhang, Nature Physics 5 (2009) 438–442.
[14] Yeping Jiang, Yilin Wang, Mu Chen, Zhi Li, Canli Song, Ke He, Lili Wang, Xi Chen, Xucun Ma, Qi-Kun Xue, Physical Review Letters 108 (2012) 016401.
[15] C. Pauly, G. Bihlmayer, M. Liebmann, M. Grob, A. Georgi, D. Subramaniam, M.R. Scholz, J. Sánchez-Barriga, A. Varykhalov, S. Blügel, O. Rader, M. Morgenstern, Physical Review B 86 (2012) 235106.
[16] Guang Wang, Xiegang Zhu, Jing Wen, Xi Chen, Ke He, Lili Wang, Xucun Ma, Ying Liu, Xi Dai, Zhong Fang, Jinfeng Jia, Qikun Xue, Nano Research 3 (12) (2010) 874–880.
[17] V.V. Atuchin, V.A. Golyashov, K.A. Kokh, I.V. Korolkov, A.S. Kozhukhov, V.N. Kruchinin, S.V. Makarenko, L.D. Pokrovsky, I.P. Prosvirin, K.N. Romanyuk, O.E. Tereshchenko, Crystal Growth and Design 11 (12) (2011) 5507–5514.
[18] K. Miyamoto, A. Kimura, T. Okuda, H. Miyahara, K. Kuroda, H. Namatame, M. Taniguchi, S.V. Eremeev, T.V. Menshchikova, E.V. Chulkov, K.A. Kokh, O. E. Tereshchenko, Physical Review Letters 109 (2012) 166802.
[19] S. Schulz, S. Heimann, J. Friedrich, M. Engenhorst, G. Schierning, W. Assenmacher, Chemistry of Materials 24 (2012) 2228–2234.
[20] D. Niesner, Th. Fauster, S.V. Eremeev, T.V. Menshchikova, Yu.M. Koroteev, A.P. Protogenov, E.V. Chulkov, O.E. Tereshchenko, K.A. Kokh, O. Alekperov, A. Nadjafov, N. Mamedov, Physical Review B 86 (2012) 205403.
[21] Guolin Hao, Xiang Qi, Yinping Fan, Lin Xue, Xiangyang Peng, Xiaolin Wei, Jianxin Zhong, Applied Physics Letters 102 (2013) 013105.
[22] C. Paorici, G. Attolini, Progress in Crystal Growth and Characterization of Materials 48–49 (2004) 2–41.
[23] V.V. Atuchin, V.G. Kesler, V.V. Ursaki, V.E. Tezlevan, Solid State Communications 138 (2006) 250–254.
[24] Desheng Kong, Wenhui Dang, Judy J. Cha, Hui Li, Stefan Meister, Hailin Peng, Zhongfan Liu, Yi Cui, Nanoletters 10 (2010) 2245–2250.
[25] V.V. Atuchin, T.A. Gavrilova, T.I. Grigorieva, N.V. Kuratieva, K.A. Okotrub, N.V. Pervukhina, N.V. Surovtsev, Journal of Crystal Growth 318 (2011) 987–990.
[26] M. Schöneich, M.P. Schmidt, P. Schmidt, Zeitschrift fuer Anorganische und Allgemeine Chemie 636 (9–10) (2010) 1810–1816.
[27] Y. Takagaki, B. Jenichen, U. Jahn, M. Ramsteiner, K.-J. Friedland, J. Lähnemann, Semiconductor Science and Technology 26 (2011) 125009.
[28] V.V. Atuchin, T.A. Gavrilova, K.A. Kokh, N.V. Kuratieva, N.V. Pervulhina, N.V. Surovtsev, Solid State Communications 152 (2012) 1119–1122.
[29] K.A. Kokh, Yu.M. Andreev, V.A. Svetlichnyi, G.V. Lanskii, A.E. Kokh, Crystal Research and Technology 46 (4) (2011) 327–330.
[30] V. Piacente, P. Scardala, D. Ferro, Journal of Alloys and Compounds 178 (1992) 101–115.
[31] Bruker AXS Inc. APEX2 (Version 1.08), SAINT (Version 7.03), and SADABS (Version 2.11). Bruker Advanced X-ray Solutions, Madison, Wisconsin, USA, 2004.
[32] C. Burla, R. Caliandro, M. Camalli, B. Carrozzini, G.L. Cascarano, L. De Caro, C. Giacovazzo, G. Polidori, R. Spagna, Journal of Applied Crystallography 38 (2) (2005) 381–388.
[33] G.M. Sheldrick, SHELX97 Release 97-2, University of Göttingen, Germany, 1998.
[34] V.V. Atuchin, O.D. Chimitova, T.A. Gavrilova, M.S. Molokeev, Sung-Jin Kim, N.V. Surovtsev, B.G. Bazarov, Journal of Crystal Growth 318 (2011) 683–686.
[35] E.V. Alekseev, O. Felbinger, S. Wu, T. Malcherek, W. Depmeier, G. Modolo, T.M. Gesing, S.V. Krivovichev, E.V. Suleimanov, T.A. Gavrilova, L.D. Pokrovsky, A.M. Pugachev, N.V. Surovtsev, V.V. Atuchin, Journal of Solid State Chemistry 204 (2013) 59–63.
[36] V.V. Atuchin, O.D. Chimitova, S.V. Adichtchev, B.G. Bazarov, T.A. Gavrilova, M.S. Molokeev, N.V. Surovtsev, Zh.G. Bazarova, Materials Letters 106 (2013) 26–29.
[37] T.L. Anderson, H.B. Krause, Acta Crystallographica B 30 (1974) 1307–1310.
[38] Yanmei Ma, Guangtao Liu, Pinwen Zhu, Hui Wang, Xin Wang, Qiliang Cui, Jing Liu, Yanming Ma, Journal of Physics: Condensed Matter 24 (2012) 475403.
[39] Tadashi C. Ozawa, Sung J. Kang, Journal of Applied Crystallography 37 (2004) 679.
[40] P. Dutta, D. Bhoi, A. Midya, N. Khan, P. Mandal, S. Shanmukharao Samathan, V. Ganesan, Applied Physics Letters 100 (2012) 251912.
[41] W. Richter, H. Köhler, C.R. Becker, Physica Status Solidi B 84 (1977) 619–628.
[42] O. Gomis, R. Vilaplana, F.J. Manjón, P. Rodríguez-Hernández, E. Pérez-González, A. Muñoz, V. Kucek, C. Drasar, Physical Review B 84 (2011) 174305.
[43] K.M.F. Shahil, M.Z. Hossain, V. Goyat, A.A. Balandin, Journal of Applied Physics 111 (2012) 054305.
[44] S.M. Souza, D.M. Trichës, J.C. de Lima, T.A. Grandi, R.S. de Biasi, Physica B 405 (2010) 2807–2814.
[45] Yuwei Li, Vladimir A. Stoica, Lynn Endicott, Guoyu Wang, Ctirad Uher, Roy Clarke, Applied Physics Letters 97 (2010) 171908.